J|A|C|S
ARTICLES
Published on Web 10/20/2006

Rates of Oxygen Exchange between the $[H_xNb_6O_{19}]^{8-x}_{(aq)}$ Lindqvist Ion and Aqueous Solutions

Jay R. Black,[†] May Nyman,[‡] and William H. Casey*,[†]

Contribution from the Departments of Chemistry and Geology, University of California, Davis, California 95616, and Geochemistry Division, Sandia National Laboratories, Albuquerque, New Mexico 87185

Received August 8, 2006; E-mail: whcasey@ucdavis.edu

Abstract: Oxygen-isotope-exchange rates were measured between sites in the Lindqvist-type $[H_xNb_6O_{19}]^{8-x}_{(aq)}$ polyoxoanion and aqueous solution as a function of pH and temperature. The ion has a central μ_6-O that is inert to exchange, 12 μ_2-O(H), and 6 η-O. The potassium salt of this ion is recrystallized in ^{17}O-enriched water to ^{17}O-label the anion, which is then redissolved into isotopically normal water so that the ^{17}O NMR signals from structural oxygens can be followed as a function of time. Because the central μ_6-O retains its ^{17}O signal throughout the experiments, it is clear that the polyoxoanion remains intact during isotopic equilibration of the other structural oxygens. At pH conditions where the $[HNb_6O_{19}]^{7-}$ ion predominates, the μ_2-O(H) sites isotopically exchange with solution about an order of magnitude more rapidly than the η-O sites. Yet, we observe that the terminal and bridging oxo sites react at nearly the same rates when the ion is coordinated to 2−3 protons and possibly when it is unprotonated. On the basis of molecular models and experimental kinetic data, we propose metastable polymorphs of the hexaniobate structure where four of the μ_2-O(H) and η-O sites are temporarily equivalent and bonded to a coordinatively unsaturated Nb(V). This hypothesized intermediate allows facile access to bulk water molecules for exchange but cannot fully explain the kinetic results and additional experiments on other Lindvist ions are required.

1. Introduction

Oxygen-isotope-exchange reactions in nanometer-size clusters are particularly interesting because the reactions are elementary or near elementary and lend themselves to computer simulation, and thus we can improve our ability to predict reaction dynamics by coupling experiments and simulation. Information about oxygen-isotope exchanges are also particularly important for understanding aqueous reactions involving minerals and extended structures, such as the dissolution of oxide materials. In these materials, the rates commonly scale with interfacial concentrations, like net proton densities at the surface, but little molecular detail is known. This sort of molecular detail can be obtained from discrete aqueous clusters, like the Lindqvist ion,[1] in ways that are impossible for more complex materials. Previous work on aqueous cluster ions has shown that some pathways for isotope exchange are strikingly counterintuitive, whereas others are relatively simple.[2,3] The replacement of bridging hydroxyls in the series of ϵ-Keggin $MO_4Al_{12}(OH)_{24}(H_2O)_{12}^{7/8+}$ (MAl_{12}) ions provides a good example. The rates for isotope exchange at the μ_2-OH bridges in these ions span a range at least as large as $\sim 10^7$ depending upon the metal (M = Al(III), Ga(III), or Ge(IV)) that is substituted into the inert core.[3] These central metals control the reaction because they affect the extent to which a metastable dimer-like transient $>Al-(\mu_2\text{-}OH)_2-Al<$ forms that is required for oxygen-isotope exchange. A strong bond to the central metal atom enhances formation of this dimer-like structure, and a weak bond suppresses it. Rates of exchange of bound water molecules, in contrast, are nearly constant across the series.[3]

Here we extend this work and examine oxygen-isotope-exchange reactions in a hexaniobate $[H_xNb_6O_{19}]^{8-x}_{(aq)}$ ion of the Lindqvist structure that has a central μ_6-O site, 12 μ_2-O bridges, and 6 terminal η-O sites (Figure 1). As with MAl_{12} ions, there is an inert core to the structure that can be identified, and followed, by ^{17}O NMR in solution so that it is clear that the oxygen-exchanges proceed on an intact molecule in solution. The Lindqvist structures have the stoichiometry $[H_xM_6O_{19}]^{(8-x)-}$ where M = Nb(V), Ta(V), and $0 \le x \le 3$, and $[M_6O_{19}]^{2-}$ where M = W(VI), Mo(VI). Chemists used these ions in early studies of ^{17}O NMR because they are so stable in aqueous solution and because they can be synthesized with ^{17}O in all sites.[4−8] The Lindqvist ions have also attracted recent attention by computational modelers[9−13] because of the ion's symmetry and its broad similarity as a polyoxometalate to nanometer-size catalysts.

[†] University of California.
[‡] Sandia National Laboratories.

(1) Lindqvist, I. *Arkiv för Kemi* **1953**, *5*, 247.
(2) Rustad J. R.; Loring J. S.; Casey W. H. *Geochim. Cosmochim. Acta* **2004**, *68* (14), 3011.
(3) Casey, W. H. *Chem. Rev.* **2006**, *106*, 1.
(4) English, A. D.; Jesson, J. P.; Klemperer, W. G.; Mamouneas, T.; Messerle, L.; Shum, W.; Tramontano, A. *J. Am. Chem. Soc.* **1975**, *97*, 4785.
(5) Filowitz M.; Ho R. K. C.; Klemperer W. G.; Shum W. *Inorg. Chem.* **1979**, *18*, 93.
(6) Nyman M.; Bonhomme F.; Alam T. M.; Rodriguez M. A.; Cherry B. R.; Krumhansl J. L.; Nenoff T. M.; Sattler, A. M. *Science* **2002**, *297*, 996.
(7) Pope M. T. *NATO Sci. Ser., II: Math., Phys. Chem.* 98 **2003**, (Polyoxometalate Molecular Science), 3−31.
(8) Pope M. T. *Comprehensive Coordination Chemistry II*; Elsevier: New York, 2004; Vol. 4, p 635.

10.1021/ja065529w CCC: $33.50

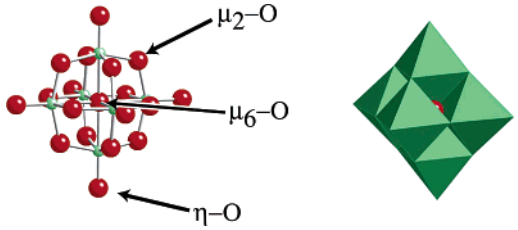

Figure 1. $[Nb_6O_{19}]^{8-}$ ion shown in ball-and-stick (left) and polyhedral (right) representation. The structure has a central μ_6-O sites that is inert to exchange, 12 μ_2-O bridges, and 6 terminal η-O sites. The central μ_6-O site is shown as a red sphere in the polyhedral representation (right). In the ball-and-stick representation, the oxygens are red and the Nb(V) metals are green.

Oxygen-exchange data on the Lindqvist ions, however, were surprisingly sparse until recent measurements of the lifetimes for exchange of the various structural oxygens at self-buffering pH conditions ($11 < pH < 12$).[14,15] These qualitative studies showed that the hexaniobate ($[H_xNb_6O_{19}]^{(8-x)-}$) ion reacts sufficiently slowly, and over a broad enough pH and temperature range, that detailed ^{17}O NMR investigations of the reaction pathways are possible. Here we extend this work by conducting a quantitative study of the rates of oxygen-isotope exchange between sites in the Lindqvist structure and bulk solution. Because the $[H_xNb_6O_{19}]^{(8-x)-}$ ion undergoes stepwise protonations of the μ_2-O bridges over the pH range of 14 to 9 (Figure 2), it also provides the opportunity to investigate the significant effect of protonation on exchange rates.

2. Experimental Methods

2.1. Synthesis. A 16-gram sample of $[K_8Nb_6O_{19}]\cdot 16H_2O$ salt was synthesized using a previously developed method.[15] This solid was ^{17}O-enriched by hydrothermal treatment of ~1.2 g of solid in ~1 mL of $H_2{}^{17}O$, followed by heating at 95 °C for 2 days in the sealed Teflon cup of a Parr reaction vessel. The crystals were then slowly recrystallized from the $H_2{}^{17}O$ solution by cooling and then physically separated from the ^{17}O-enriched water using a vacuum line.

2.2. pH Measurements. The pH of each experimental solution (Table 1) was estimated in two ways. First, the pH was measured on the concentration scale using a glass combination electrode that had been calibrated by Gran titration using a standard acid at the appropriate temperature. The ionic strength and composition of this solution was matched to the samples as closely as possible. The accuracy of these pH estimates was checked by comparing the measured pH to those of standards with known hydroxide-ion concentration and no hexaniobate ion in the background electrolyte. In general, these pH estimates were within ~0.15 unit of one another. The pH values were also calculated using the excess hydroxide ion concentrations in samples where excess KOH was added to adjust the pH (Table 1). Calculations at our experimental conditions (3 M KCl) were possible because the conditional association constants for the protonation of the hexaniobate ion ($\beta_1 = K_1 = 13.63$, $\beta_2 = 23.55$, and $\beta_3 = 32.90$ at 298 K in 3 M KCl)[16] and dissociation of water[19] are also reported for these conditions. The β_i are conditional equilibrium constants for protonation of the $[Nb_6O_{19}]^{8-}$ ion with 'i' protons to form the $[H_iNb_6O_{19}]^{(8-i)-}$ ion. In general, the pH estimates from the calculations are also within ~0.15 unit of our experimental estimates.

2.3. NMR Spectroscopy. The solution-state ^{17}O NMR experiments were conducted with a Bruker Avance spectrometer located at the UCD NMR facility. This spectrometer is based on an 11.7 T magnet ($\nu_o =$ 67.8 MHz for ^{17}O) and is fitted with a 10-mm broadband probe. The ^{17}O NMR spectra were taken with single-pulse excitation using 20 μs pulses ($\pi/2 \approx 40$ μs) and recycle delays of 6 ms. Depending upon the sample, 1000−40 000 acquisitions were required to establish adequate signal-to-noise ratios. The time-domain data were digitized at 100 kHz. We used only Teflon-lined NMR tubes to prevent corrosion of the glass. The temperatures were checked by placing a copper−constantan thermocouple into the sample tube and inserting this apparatus into the spectrometer. The precision and accuracy of the temperature setting is equal to, or better than, ±0.5 K.

2.4. ^{17}O-Exchange Studies. A series of samples (Table 1) was prepared to measure the rate of exchange of oxygen sites as a function of concentration, pH, and temperature. An experiment is typically begun by dissolving ^{17}O-enriched $[K_8Nb_6O_{19}]\cdot 16H_2O$ crystals into isotopically normal water that had been prepared to reach a target pH after dissolution and hydrolysis of the ion. Typically, a few tens of milligrams of enriched solid was dissolved into 2 mL of isotopically normal water. Proton uptake by the $[Nb_6O_{19}]^{8-}{}_{(aq)}$ ion typically causes the solution pH to rise to pH ≈ 12.4 as the salt dissolves. Higher pH conditions were reached by adding small amounts of 3 M KOH and lower pH conditions were reached by adding potassium borate or potassium carbonate buffers to the solution (Table 1). These anionic buffers were chosen because they would presumably interact less with the anionic niobate ion than cationic buffers, such as amines. The apparent ionic strength was maintained at 3 M by addition of KCl to the solutions.

Immediately upon dissolution of the niobate salt into isotopically normal solution, conspicuous peaks are evident near 630 ppm, near 375 ppm, near 35 ppm, and near 0 ppm (Figure 3). Before the relative intensities change by reaction, the integrated areas of the peaks vary in an approximate ratio of 6:12:1, consistent with the assignment of the peak near 630 ppm to the six equivalent η-O sites in the $[H_xNb_6O_{19}]^{(8-x)-}$ ion, the peak near 375 ppm to the twelve μ_2-O sites, and the peak near 35 ppm to the single μ_6-O site.[4−6,14−15] The location of these peaks, and the line widths, vary with pH (Figure 4), but at a constant pH, the peak widths and positions do not change with elevated temperatures from 5 to 55 °C. The peak near 0 ppm is assignable to bulk water.

The ^{17}O NMR signals for the bridges and terminal sites decrease with time as they exchange oxygen isotopes with bulk solution (Figure 3),[14,15] yet the intensity of the ^{17}O NMR signal from the central μ_6-O site remains constant, indicating that the $[H_xNb_6O_{19}]^{8-x}{}_{(aq)}$ anion does not dissociate as the other structural oxygens equilibrate. At pH conditions where a fraction of the μ_2-O sites are protonated to form μ_2-OH, protons exchange so rapidly between the μ_2-O and μ_2-OH sites that only a single ^{17}O NMR peak is observed. Because the μ_2-O and μ_2-OH sites are in rapid-exchange equilibrium and cannot be distinguished, in subsequent discussion we refer to them as μ_2-O(H) sites, since the largest fraction of bridging oxygens on the anion remain unprotonated. The decline in intensity of the ^{17}O peaks as a function of time yields rates of isotopic exchange for the η-O and μ_2-O(H) sites and, at ambient conditions, the μ_6-O is inert to exchange.

3. Results

3.1. Rates of Isotopic Equilibration. In all cases, the ^{17}O NMR signals from the η-O and μ_2-O(H) sites decrease

(9) Bridgeman, A. J.; Cavigliasso, G. *Inorg. Chem.* **2002**, *41*, 1761.
(10) Li, J. *J. Cluster Sci.* **2002**, *13*, 127.
(11) Poblet, J. M.; Lopez, X.; Carles, B. *Chem. Soc. Rev.* **2003**, *32*, 297.
(12) Rohmer, M.-M.; Marc, B. *Dalton Trans.* **2003**, *18*, 3587.
(13) Lopez, X.; Weinstock, I. A.; Bo, Carles, Sarasa, J. P.; Poblet, J. M. *Inorg. Chem.* **2006**, *45*, 6467.
(14) Alam, T. M.; Nyman, M.; Cherry B. R.; Segall J. M.; Lybarger, L. E. *J. Am. Chem. Soc.* **2004**, *126*, 5610.
(15) Nyman M.; Alam T. M.; Bonhomme F.; Rodriquez M. A.; Frazer C. S.; Welk M. E. *J. Cluster Sci*. **2006**, *17*, 197.
(16) Etxebarria N.; Fernandez L. A.; Madariaga J. M. *Dalton Trans.* **1994**, *20*, 3055.
(17) Rozantsev G. M.; Dotsenko O. I.; Taradina G. V. *Russ. J. Coord. Chem. (Translation of Koord. Khim.)* **2000**, *26*, 247.
(18) Goiffon, A.; Granger, R.; Bockel, C.; Spinner, B. *Rev. Chim. Min.* **1973**, *10*, 487.
(19) Harned, H. S.; Hamer, W. J. *J. Am. Chem. Soc*. **1933**, *55*, 2194.

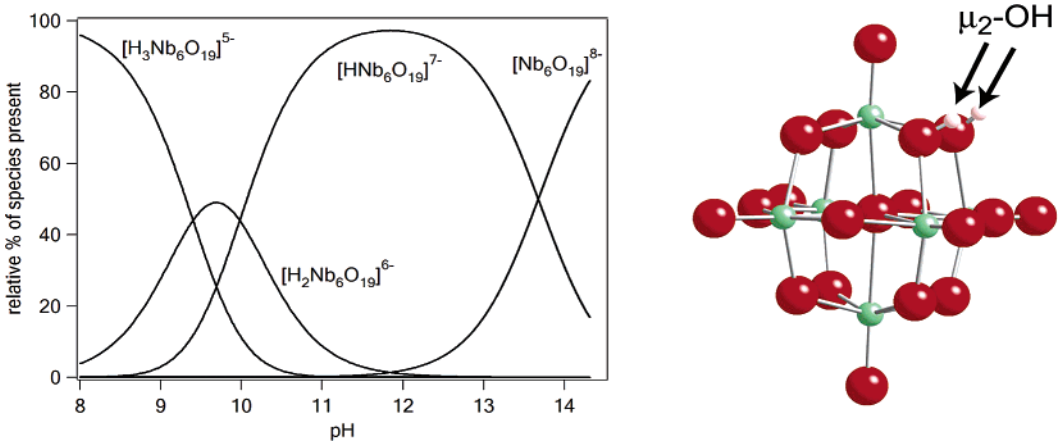

Figure 2. (Left) Speciation of the $[H_xNb_6O_{19}]^{(8-x)-}$ ion at 298 K and 3.0 M KCl at $\Sigma Nb(V) = 0.12$ M.[16−18] The conditional equilibrium constants correspond to 3.0 M KCl.[16] (Right) Proton positions have been determined in crystals by X-ray and MAS NMR methods. This $[H_2Nb_6O_{19}]^{6-}$ cluster is taken from a $Rb_6H_2Nb_6O_{19}\cdot 19(H_2O)$ crystal from Nyman et al.[15] In solution at room temperature, the μ_2-OH and μ_2-O bridges interconvert rapidly on the NMR time scale and the two sites would not be distinguishable in ^{17}O NMR. In the ball-and-stick representation, the oxygens are red and the Nb(V) metals are green.

Table 1. Sample Compositions and Rate Data[a]

sample	temp, °C	measured pH	calculated pH	$[H_xNb_6O_{19}]^{(8-x)-}$ mM	$[OH^-]$ M	$[K^+]$ M	$[Cl^-]$ M	$[CO_3^{2-}]$ M	$[BO_3^{3-}]$ M	log(τ) μ_2-O(H)	log(τ) η-O
46_100	4.1	10.38		20.0		3.16	2.96	0	0.086	3.22	3.15
46_101	4.1	10.65		20.2		3.16	2.97	0	0.062	3.68	3.60
46_102	4.1	11.34		19.2		3.11	2.12	0.415	0	4.71	4.77
46_105	4.1	10.34		13.1		3.11	2.98	0	0.043	3.64	3.25
46_30	15.9	14.29	14.36	20.5	0.940	3.16	1.99	0	0	5.06	5.49
46_38	15.9	11.06		20.8		3.12	2.12	0.415	0	4.13	4.26
46_39	15.9	12.40		21.0		3.17	3.00	0	0	4.65	5.49
46_49	15.9	11.36		20.7		3.16	2.50	0.250	0	4.39	4.77
46_54	15.9	10.13		21.4		3.17	2.96	0	0.086	2.74	2.72
46_55	15.9	10.25		20.7		3.17	2.97	0	0.068	2.99	2.94
46_56	15.9	10.36		21.3		3.17	2.97	0	0.068	2.94	2.96
46_71	15.9	13.33	13.38	21.0	0.098	3.17	2.89	0	0	4.69	5.58
46_75	15.9	12.96	12.93	20.7	0.035	3.16	2.96	0	0	4.69	5.62
48_66	15.9	14.72	14.83	20.4	2.806	3.16	0.00	0	0	5.53	5.54
46_82	24.4	12.25		20.8		3.17	3.00	0	0	4.13	5.09
46_83	24.4	13.12	13.04	21.1	0.098	3.17	2.89	0	0	4.21	5.14
46_85	24.4	13.99	14.02	20.3	0.940	3.16	1.99	0	0	4.54	5.06
46_86	24.4	12.64	12.49	20.8	0.028	3.17	2.97	0	0	4.18	5.15
46_87	24.4	13.53	13.37	20.5	0.211	3.16	2.77	0	0	4.31	5.08
46_88	24.4	13.68	13.67	20.3	0.421	3.16	2.55	0	0	4.36	5.06
46_93	24.4	14.44	14.49	20.0	2.806	3.16	0.00	0	0	4.93	5.03
46_94	24.4	11.12		20.5		3.12	2.12	0.415	0	3.84	4.11
46_95	24.4	11.23		21.0		3.16	2.50	0.250	0	3.90	4.29
46_107	24.4	11.74		10.2		3.16	3.00	0.038	0	4.05	4.90
46_108	24.4	10.43[b]		14.0		3.11	2.98	0	0.033	2.78	2.77
46_111	24.4	13.06	13.04	13.6	0.098	3.11	2.89	0	0	4.23	5.17
46_112	24.4	13.04	13.04	3.4	0.098	3.03	2.89	0	0	4.24	5.22
46_113	24.4	13.05	13.04	6.9	0.098	3.06	2.89	0	0	4.21	5.18
46_96	30.3	12.92	12.82	20.7	0.098	3.16	2.89	0	0	3.89	4.86
48_68	30.3	14.21	14.11	20.1	2.806	3.16	0.00	0	0	4.59	4.70
46_106	35.5	12.75	12.71	9.2	0.112	3.07	2.88	0	0	3.65	4.52
48_67	35.5	14.05	14.28	20.0	2.806	3.16	0.00	0	0	4.31	4.44
46_115[c]	24.4		13.04	20.6	0.098	3.16	2.89	0	0		
46_115[d]	24.4	14.53		14.4		5.20	2.03	0	0		
46_116[c]	24.4		13.04	20.4	0.098	3.16	2.89	0	0		
46_116[d]	24.4	10.80		20.4		4.05	2.89	0.495	0		

[a] The τ values are in seconds, and the precision of the pH measurements is ±0.15 unit based upon measured and calculated values. Uncertainties in the concentrations are ±1 percent. [b] pH estimated from dummy sample. [c] Sample composition before pH adjustment. [d] Sample composition after decay of the signal from the μ_2-O(H) and further adjustment of pH.

exponentially with time (e.g., Figure 5). These variations in the Lorentzian peak areas as a function of time were fit to eq 1 to estimate the characteristic times (τ) for reaction:

$$I(t) = I_0\, e^{-t/\tau} \qquad (1)$$

where I_0 is the initial intensity, which is treated as an adjustable parameter, t is time in seconds, and τ is a characteristic time (seconds) for isotopic exchange and elimination of the ^{17}O NMR signal. The values of τ for of the η-O and μ_2-O(H) sites vary considerably with pH and temperature, although we observe no dependence of values of τ on the total niobate concentration (Table 1). The chemical shifts of the η-O, μ_2-O(H), and μ_6-O peaks vary as a function of pH (Figure 4). As the pH increases from 10 to 14.5, signals from the η-O and μ_6-O sites shift upfield

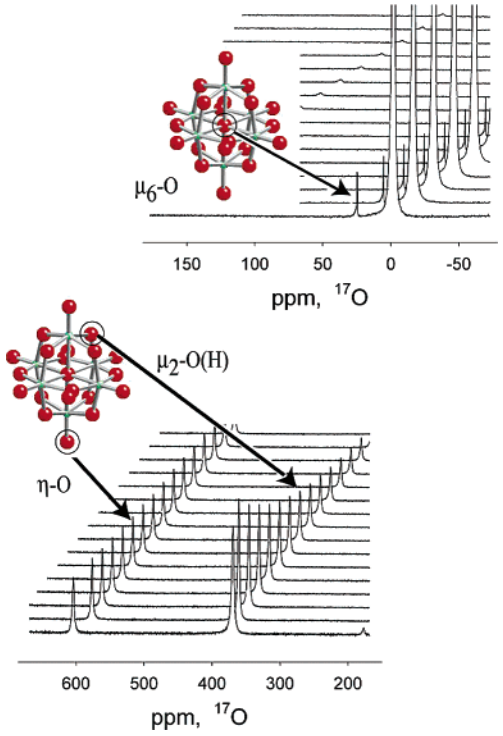

Figure 3. Different oxygen sites in the $[H_xNb_6O_{19}]^{(8-x)-}$ ion yield distinct peaks in the ^{17}O NMR spectra. The structure, shown in ball-and-stick representation, was initially enriched in ^{17}O so the intensity of the peaks decrease with time as structural oxygens exchange with bulk solution. The peak labels are: η-O, μ_6-O, μ_2-O(H).[4−6,14−15] The μ_6-O site (top), 12 μ_2-O bridges, and 6 terminal η-O sites (bottom) have the approximate intensity ratio of 1:12:6, as expected from the stoichiometry.

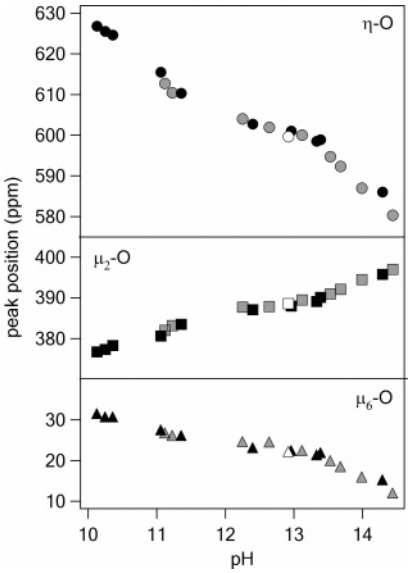

Figure 4. Variation in ^{17}O NMR peak positions with pH at 277 K (black symbols), 298 K (grey symbols), and 303 K (hollow symbols) for the η-O (top), μ_2-O(H) (middle), and μ_6-O (bottom).

by ~40 ppm and ~20 ppm, respectively, whereas the signal from the μ_2-O(H) site shifts downfield ~20 ppm.

The variation of rates with pH is complicated, and three regions (labeled **A**, **B**, and **C** in Figure 6) are discussed separately. In the region labeled **A**, at pH < 11 and constant temperature, the rates of exchange of the η-O and μ_2-O(H) sites are virtually identical and $-\log(\tau)$ decreases linearly with decreasing pH. We observe no dependence of the oxygen

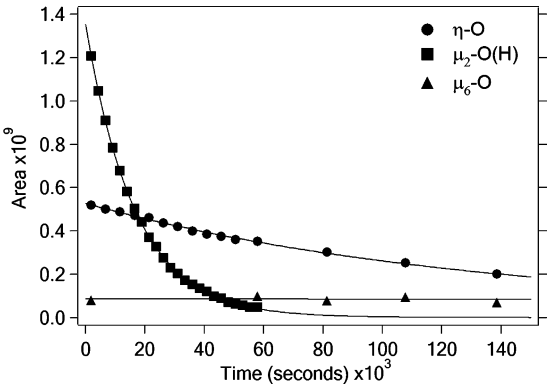

Figure 5. Variation in the ^{17}O NMR peak intensity (integrated area) for sample 46_111. ΣNb(V) = 0.082 M at pH = 13.06 and 297.53 K. The signals for the μ_2-O(H) and the η-O decrease exponentially with time as the intensity of the signal from the μ_6-O is constant, indicating that the ion remains intact as the structural oxygens exchange isotopes with bulk solution.

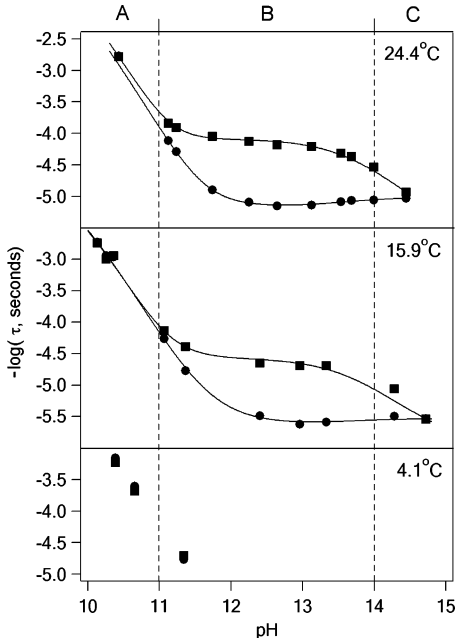

Figure 6. Rates of oxygen-isotope exchange, expressed as τ, from the η-O (●) and μ_2-O(H) (■) sites of the $[H_xNb_6O_{19}]^{(8-x)-}$ ion as a function of pH. The solid lines represent fits of a rate law to the data (see Section 4.1 in text). Note that the values of τ become equal for the two sites at very high pH and at pH < 11 and that there is no distinct pH dependence for exchange of oxygen at the η-O sites (●) in the pH range 12 < pH < 14.4, but the rates of exchange of oxygens in the μ_2-O(H) sites exhibit a slow, but distinct variation with pH. The regions labeled **A**, **B**, and **C** are discussed separately in the text.

exchange rate on the total concentration of $[H_xNb_6O_{19}]^{(8-x)-}$ ion at 24.4 °C and pH 13 ($\log \tau_{\eta-O} = 5.18 \pm 0.07$; $\log \tau_{\mu2-O(H)} = 4.22 \pm 0.03$, see samples 46_83, 46_111, 46_112, and 46_113 in Table 1).

In the pH region 11 < pH < 14 (labeled **B** in Figure 6), the characteristic times for isotopic exchange of the η-O and μ_2-O(H) sites differ considerably from one another, and the monoprotonated $[HNb_6O_{19}]^{7-}$ ion predominates in solution (Figure 2). The η-O site is about an order of magnitude less reactive than the μ_2-O(H) site at a fixed pH and temperature. The η-O site exhibits small dependence on pH, whereas τ values for the μ_2-O(H) site decrease slowly with pH until the rates become equal to the η-O site at pH = 14.4 (labeled **C** in Figure 6).

Table 2. Activation Enthalpies and Entropies for Oxygen Exchange from Water with the η-O and μ_2-O(H) Sites of the Hexaniobate Ion as a Function of pH

	η-O		μ_2-O(H)	
pH	$\Delta H^{\ddagger} \pm 2\sigma$ (kJ mol^{-1})	$\Delta S^{\ddagger} \pm 2\sigma$ (J mol^{-1} K^{-1})	$\Delta H^{\ddagger} \pm 2\sigma$ (kJ mol^{-1})	$\Delta S^{\ddagger} \pm 2\sigma$ (J mol^{-1} K^{-1})
~13	91.9 ± 4.8	210 ± 16	90.5 ± 2.8	224 ± 9.3
~14.5	96.3 ± 2.0	227 ± 6.7	107 ± 7.4	263 ± 25

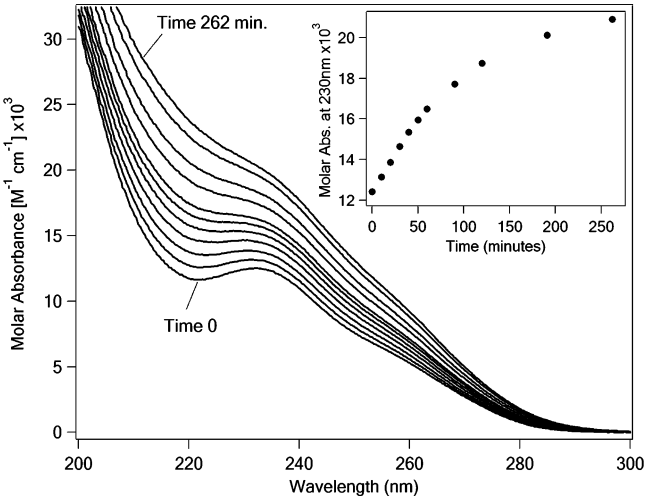

Figure 7. UV−vis spectra over time of the hexaniobate ion (0.02 M) buffered with potassium borate (0.5 M) to pH 8.5. (Inset) Exponential increase in the absorbance at 230 nm with time.

The rate coefficients from the variable-temperature experiments yield the activation enthalpy ($\Delta H^{\ddagger}$) and entropy ($\Delta S^{\ddagger}$) via the Eyring equation (eq 2).

$$\frac{1}{\tau} = \frac{k_B T}{\hbar} e^{-[(\Delta H^{\ddagger} - T\Delta S^{\ddagger})/RT]} \quad (2)$$

The term k_B is Boltzmann's constant, T is the experimental temperature in Kelvin, $\hbar$ is Planck's constant, and R is the gas constant. Table 2 summarizes the calculated activation enthalpies and entropies from least-squares fits of the data to eq 2 at pH $\approx$ 13 and 14.5. Because a fraction of the bridges are protonated (pK_{a3} = 13.63; Figure 2), there is a small contribution to the experimental activation energy from the enthalpy of protonation of bridging oxygens on the anion. Correspondingly, the values of $\Delta H^{\ddagger}$ are virtually constant with pH for the unprotonated η-O site (96.3 ± 2.0 kJ/mol at pH = 14.4; 91.9 ± 2.8 kJ/mol at pH = 13; Table 2), but decrease slightly with pH for the μ_2-O(H) sites (107 ± 7.4 kJ/mol at pH = 14.4 to 90.5 ± 2.8 at pH = 13). The contribution must be small, because these activation parameters are typical for unenhanced bond ruptures in oxide ions.[20]

3.2. Evidence for Oligomerization of the $[H_xNb_6O_{19}]^{(8-x)-}$ Ion at Low pH. We observe slow transformation of the Lindqvist $[H_xNb_6O_{19}]^{(8-x)-}$ ion in the UV−vis spectra at low pH, which is evident as the decay of the hexaniobate peak (230 nm, Time 0, Figure 7) and the formation of a broad absorption shoulder (Time 262 min, Figure 7). This growth was originally identified and was later interpreted to indicate slow linkage of $[H_xNb_6O_{19}]^{(8-x)-}$ ions.[18,21] We, too, interpret these observations to indicate that the $[H_xNb_6O_{19}]^{(8-x)-}$ ion is oligomerizing and that the reaction is sensitive to pH. Larger oligomers are evident in a capillary-electrophoresis scan of the solutions. Although we could not assign firm stoichiometries, we suspect that the changes indicate nearly intact condensation of two $[H_xNb_6O_{19}]^{(8-x)-}$ ions to form a larger dimer-like structures, perhaps similar to the $[Nb_{10}O_{28}]^{6-}$ moiety[22] or the recently reported $[Nb_{20}O_{54}]^{8-}$ moiety synthesized using nonaqueous solvents.[23] This oligomerization does not affect our rate measurements, most of which are at much higher pH conditions where oligomerization occurs on a negligible time scale.

4. Discussion

There are key points to summarize from the results. First, rates of isotopic exchange of the η-O and μ_2-O(H) sites with bulk solution become virtually equal to one another at low pH (<11) and possibly at high pH (~14.4) (regions **A** and **C** in Figure 6), although we do not have extensive rate measurements at pH>14 to confirm this point. At the highest pH, the hexaniobate ion is virtually deprotonated and at the lower pH conditions, it has 2−3 protons, which are probably on the bridging oxygens. Second, in the intermediate pH-region (**B** in Figure 6), where the $[HNb_6O_{19}]^{7-}$ ion predominates, the rates of isotopic exchange of the η-O and μ_2-O(H) sites differ considerably, with the η-O sites reacting more slowly than the μ_2-O(H) sites. Reaction of the η-O site exhibits virtually no pH dependence in this pH region whereas the rates of exchange of the μ_2-O(H) sites, a fraction of which are protonated, decrease steadily with pH.

These kinetic data are consistent with our understanding of protonation of the hexaniobate ion. The sites of protonation of the hexaniobate anion in solution are most likely the μ_2-O bridges and not the terminal oxygens, consistent with protonation observed in the solid state via X-ray structural studies[15,24] and MAS NMR[14] of the salts. In some cases for the $[H_2Nb_6O_{19}]^{6-}$ ion the μ_2-OH bridges lie trans to one another across the central μ_6-O in the crystal.[24] In other cases, the μ_2-OH bridges can also form adjacent to one another (e.g. $Cs_6[H_2Nb_6O_{19}]\cdot 9(H_2O)$ and $Rb_6[H_2Nb_6O_{19}]\cdot 19(H_2O)$ salts).[15] Bridge protonation is found in other polyoxometalate ions where the η-O sites have bond orders of two or higher. The $[V_{10}O_{28}]^{6-}$ anion, for example, is structurally similar to the niobate Lindqvist ion and protonates at the bridging oxo sites rather than terminal oxygens.[7−8,25−26]

4.1. Rates of Isotopic Exchange. The simplest rate model is that the pH dependency of rate reflects changes in the protonation state of the $[H_xNb_6O_{19}]^{(8-x)-}$ ion and not changes in concentrations of OH^- or H_3O^+. Thus, exchange probably involves an isotopically normal water molecule. Such a rate law would have a form like:

$$\frac{1}{\tau} = ([H_2O])^n \sum_{i=0}^{3} k^i X_i ... \quad (3)$$

(20) Richens, D. T. *The Chemistry of Aqua Ions*; J. Wiley: New York, 1997.
(21) Goiffon A.; Spinner B. *Talanta* **1977**, *24*, 130.
(22) Graeber, E. J.; Morosin, B. *Acta Crystallogr.* **1977**, *B33*, 2137.
(23) Maekawa, M.; Ozawa, Y.; Yagasaki, A. *Inorg. Chem.* **2006**, doi: 10.1021/ic0601788.
(24) Ozeki T.; Yamase T.; Naruke H.; Sasaki Y. *Bull. Chem. Soc. Jpn.* **1994**, *67*, 3249.
(25) Day, V. W.; Klemperer W. G.; Maltbie, D. J. *J. Am. Chem. Soc.* **1987**, *109*, 2991.
(26) Evans H. T.; Pope M. T. *Inorg. Chem.* **1984**, *23*, 501.

Table 3. Optimized Rate Coefficients for the Rate Law Presented as Eq 4[a]

	η-O				μ_2-O(H)				
temp, °C	k^0	k^1	k^2	k^3	k^0	k^1	k^2	k^3	residual[b]
24.4									
1	9.695×10^{-6}	6.670×10^{-6}	1.597×10^{-4}	0.0617	1.046×10^{-6}	8.106×10^{-5}	1.804×10^{-13}	0.0831	0.12
2	9.627×10^{-5}	7.101×10^{-6}	6.605×10^{-5}	0.0777	1.047×10^{-6}	8.106×10^{-5}	8.323×10^{-14}	0.0777	0.14
3	9.626×10^{-6}	7.113×10^{-6}	2.375×10^{-5}	0.0877	6.488×10^{-7}	8.370×10^{-5}	3.922×10^{-4}	0.0438	0.26
4	1.047×10^{-5}	4.763×10^{-6}	0.001	0	2.330×10^{-6}	7.272×10^{-5}	0.0013	0	2.79
15.9									
5	2.957×10^{-6}	2.379×10^{-6}	1.853×10^{-4}	0.0306	1.023×10^{-6}	2.639×10^{-5}	1.611×10^{-4}	0.0294	0.42

[a] The superscripts refer to the protonation states of the hexaniobate ion (e.g., $k^0 = Nb_6O_{19}^{8-}$, $k^3 = H_3Nb_6O_{19}^{5-}$, etc). In Fits 1 and 5, separate rate coefficients were calculated for the terminal and bridging oxygens, and all protonated forms of the structure were included. In Fit 2, the k^3 rate coefficient for the terminal and bridging oxygens was required to be equal, and all protonated forms of the structure were included. In Fit 3, the k^3 rate coefficient for the terminal oxo sites was forced to be twice that of the bridging oxo sites, and all protonated forms of the structure were included. In Fit 4, the k^3 term was set to zero. In Fit 5, the K_a values[16] are not adjusted for the lower temperature. [b] $Residual = \sum [\log(Rate_{observed}) - \log(Rate_{calculated})]^2_{\mu_2-O(H)} + \sum [\log(Rate_{observed}) - \log(Rate_{calculated})]^2_{\eta-O}$.

where k^i are the rate coefficients for the various protonated forms of the hexaniobate ion (i.e., $i = 0-3$), and X_i is the mole fraction of total niobate in the various protonated forms; e.g.,

$$X_0 = \frac{[Nb_6O_{19}{}^{8-}]}{\sum [H_xNb_6O_{19}{}^{(8-x)-}]}$$

$$X_1 = \frac{[HNb_6O_{19}{}^{7-}]}{\sum [H_xNb_6O_{19}{}^{(8-x)-}]}$$

$$X_2 = \frac{[H_2Nb_6O_{19}{}^{6-}]}{\sum [H_xNb_6O_{19}{}^{(8-x)-}]}$$

where the subscripts refer to the number of protons on the $[H_xNb_6O_{19}]^{(8-x)-}$ ion. These mole fractions can be calculated from conditional equilibrium constants:[16]

$$x_{Nb_6O_{19}{}^{8-}} = \frac{K_{a1}K_{a2}K_{a3}}{[H^+]^3 + [H^+]^2K_{a1} + [H^+]K_{a1}K_{a2} + K_{a1}K_{a2}K_{a3}}$$

$$x_{HNb_6O_{19}{}^{7-}} = \frac{K_{a1}K_{a2}[H^+]}{[H^+]^3 + [H^+]^2K_{a1} + [H^+]K_{a1}K_{a2} + K_{a1}K_{a2}K_{a3}}$$

$$x_{H_2Nb_6O_{19}{}^{6-}} = \frac{K_{a1}[H^+]^2}{[H^+]^3 + [H^+]^2K_{a1} + [H^+]K_{a1}K_{a2} + K_{a1}K_{a2}K_{a3}}$$

$$x_{H_3Nb_6O_{19}{}^{5-}} = \frac{[H^+]^3}{[H^+]^3 + [H^+]^2K_{a1} + [H^+]K_{a1}K_{a2} + K_{a1}K_{a2}K_{a3}}$$

where

$$K_{ax} = \frac{[H_xNb_6O_{19}{}^{(8-x)-}]}{[H^+][H_{x-1}Nb_6O_{19}{}^{(9-x)-}]}$$

If we assume further that the rate orders are all unity and ignore the concentration of water, an even simpler expression results:

$$\frac{1}{\tau} = \sum_{i=0}^{3} k^i X_i ... \qquad (4)$$

that resembles somewhat the rate laws for dissolution of oxide solid surfaces.[27]

This rate law was fit to the rate data at 24.4 and 15.9 °C and the results for various assumptions are compiled in Table 3. The best fits were obtained by including all forms of the $[H_xNb_6O_{19}]^{(8-x)-}$ ion ($i = 0-3$) and by optimizing rate coefficients for both the η-O and μ_2-O(H) sites separately. The results of these fits are shown on Figure 6 as solid lines fitting the observed rate data. Although the $[H_3Nb_6O_{19}]^{5-}$ ion has not been identified by X-ray structural analysis of crystals, removal of the term in eq 4 that corresponds to this ion produces a poor fit to the data in the pH < 11 region (Fit 4, Table 3).

The analysis raises two interesting points. First, the reactivity can be adequately explained by appealing only to changes in the protonation state of the hexaniobate oxide anion. We recognize that other interpretations are possible, but this interpretation links the isotope-exchange rates on this polyoxoanion to the rate laws for dissolving oxide solids, where the entire pH dependence arises from changes in the protonation state of the surface.[27,28] It is a simple model that increases the rates of bond rupture by reasonable extents with protonation.

Second, the fact that the rate coefficient for the $[H_3Nb_6O_{19}]^{5-}$ ion is so similar for both the η-O and μ_2-O(H) sites (Fit 1, Table 3) suggests that they react equivalently in region **A** and, possibly, in region **C**, although data at pH >14 are sparse. In fact, a fit to eq 4 that requires that the rate coefficients, k^3, for the η-O and μ_2-O(H) sites are equal (Fit 2, Table 3) gives residual errors that are virtually indistinguishable from the case where these sites are fit separately to yield two separate values (Fit 1, Table 3). In contrast, if, for reasons discussed below, the values of k^3 for the η-O site are forced to be twice the value of k^3 for μ_2-O(H), the residual errors double (Fit 3 in Table 3). The most reasonable conclusion is that the terminal and bridging oxygens react at identical rates at low-pH conditions and, possibly, at the highest-pH conditions. Below we suggest that the molecule periodically undergoes a structural transition that makes the η-O and μ_2-O(H) sites transiently equivalent during the exchange events. First, however, we evaluate whether the oxygen exchanges could arise from an intrastructural rearrangement.

4.2. Test for Equivalence of the Bridging and Terminal Oxygens at Exchange. 4.2.1. Intramolecular Scrambling That Is More Rapid Than Isotopic Exchange. There is no

(27) Casey, W. H.; Sposito, G. *Geochim. Cosmochim. Acta* **1992**, *56*, 3825.
(28) Casey, W. H.; Ludwig, Chr. *Nature* **1996**, *86*, 506.

evidence for rapid intrastructural scrambling of oxygens within the hexaniobate ion even though the η-O and μ_2-O(H) sites exchange oxygen isotopes at the same rates at some pH conditions. We tested for such scrambling in two ways. First, we conducted variable-temperature ^{17}O NMR experiments to look for evidence that the ^{17}O NMR peaks assigned to the η-O and μ_2-O(H) sites were coalescing on the NMR time scale. Coalescence of the ^{17}O NMR peaks would be observed if the characteristic time for exchange between these two sites were $\tau \approx [\sqrt{2}/\pi](\nu_{\eta-O} - \nu_{\mu-O})$, where $\nu_{\eta-O}$ and $\nu_{\mu-O}$ correspond to the frequencies in Hz of the ^{17}O NMR peaks that correspond to the terminal and bridging oxygens, respectively.[29] In our case, the η-O and μ_2-O(H) must interconvert at a time scale of $\sim 10^4$ Hz or greater for us to observe incipient coalescence. We see no evidence for such rapid interconversion in our variable-temperature experiment and, once pH is rigorously controlled, we see no movement of the ^{17}O NMR peaks toward one another as temperature (and rates of any interconversion) is increased to 55 °C.

Similarly, we see no evidence for slow transfer of ^{17}O from the ^{17}O-enriched η-O sites to unenriched μ_2-O sites in experiments over hours. To prepare samples where the η-O and μ_6-O sites, but not the μ_2-O(H) sites, contain ^{17}O, we enriched a sample uniformly in ^{17}O then dissolved the salt into isotopically normal water. This solution was adjusted to a pH $\approx$ 13 using KOH and allowed to react with isotopically normal water for several hours. The difference in reactivity of the η-O and μ_2-O(H) sites is profound at this pH, so that the ^{17}O-tagged μ_2-O sites react away, leaving both the η-O and μ_6-O sites with ^{17}O enrichment. This solution was then adjusted to a target pH (pH $<$ 11; pH $\approx$ 14.4; regions **A** and **C** in Figure 6) where the η-O and μ_2-O(H) sites react at approximately equal rates and spectra were collected to see if ^{17}O was transferred to the unenriched μ_2-O(H) sites from the ^{17}O-enriched η-O. These experiments were run with a $TbCl_3$ internal standard so that changes in peak intensity of a few percent could be reliably measured.

In neither experiment did we observe an increase in intensity of the ^{17}O NMR signal from the isotopically normal μ_2-O(H) sites but, instead, observed only steady decline in the ^{17}O signal for the η-O sites (Figure 8). From these experiments we conclude that there is no steady internal exchange of η-O and μ_2-O(H) sites. In other words, the fact that the rates of isotopic exchange are equal in region **A** (and possibly in region **C** of Figure 6) suggests that the sites are probably becoming equivalent during the isotope-exchange event and not before.

4.2.2. Exchange in a Transient Metastable Structure: A Hypothesis. The Lindqvist ion structure does not dissociate during isotopic equilibration or we would observe ^{17}O signal loss from the μ_6-O site, which is unequivocally constant. Any change in the structure that leads to equivalence of the η-O and μ_2-O(H) sites must involve a concerted motion of many atoms because the structure is so compact and symmetric. However, the Lindqvist ion structure can be viewed as consisting of three mutually orthogonal rings of four Nb(V) linked by four μ_2-O(H) (Figure 1). We suggest that one of these rings opens to form a metastable structure where the η-O and μ_2-O rotate to replace one another. After exchange, we suggest that this metastable structure collapses back into the stable Lindqvist ion structure.

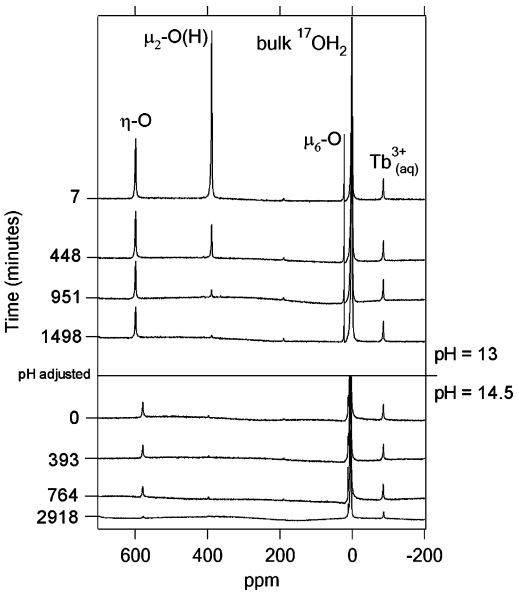

Figure 8. ^{17}O NMR spectra of a solution (46_115, Table 1) to check for transfer of ^{17}O from the labeled η-O sites to the unlabeled μ_2-O(H) sites. The first step is to allow the μ_2-O(H) sites to isotopically equilibrate with solution at pH = 13, leaving a large signal from ^{17}O-labeled η-O sites. When the signal from the μ_2-O(H) sites is virtually gone, the pH is adjusted to a region (**A** or **C**, Figure 6) where the oxygens react at similar rates. We see no evidence for transfer of ^{17}O from the η-O sites to the unlabeled μ_2-O(H) sites. The peak intensities are normalized to that of a $TbCl_3$ insert ($\sim$−100 ppm) to account for differences in the number of acquisitions and fluctuations in power.

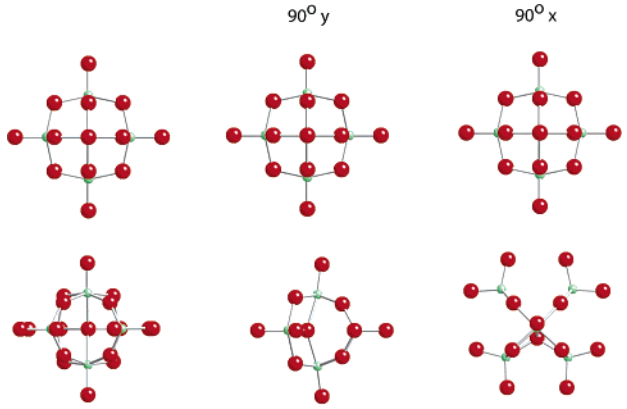

Figure 9. Two alternative structures of the $[Nb_6O_{19}]^{8-}$ ion, determined by ab initio methods (B3LYP/DGDZVP/DFT/COSMO; see S2 in Supporting Information). The conventional Lindqvist structure is shown at the top, with the structure rotated 90° about the *y* and *x* axes in the middle and rightmost columns, respectively. Our proposed metastable structure is shown on the bottom. This structure has one of the orthogonal $Nb_4(\mu_2\text{-}O)_4(\eta\text{-}O)_4$ rings opened up (bottom, right) such that the μ_2-O and η-O sites become temporarily equivalent and the coordination number of the Nb(V) temporarily decreases from six to four or five. A metastable intermediate such as this, if it were a precursor, could explain why the rates of isotopic exchange of the μ_2-O and η-O sites are equivalent at low-pH conditions and, possibly at pH > 14. The oxygens are shown in red and the Nb(V) metals in green. Similar structures can be identified with variously protonated oxygens.

One proposed metastable structure, where bridging and terminal oxygen sites become equivalent, is shown in Figure 9 as a fully deprotonated ion, along with the stable Lindqvist ion structure, with both structures rotated to show the displacements. The Lindqvist ion structure, of course, is cubically symmetric

(29) Harris, R. K. *Nuclear Magnetic Resonance Spectroscopy*; Longman Scientific: New York, 1986.

and such rotations produce equivalent structures. Rotation of the metastable structure, which is partly opened, shows that two of the three orthogonal $Nb_4(\mu_2\text{-}O(H))_4(\eta\text{-}O)_4$ rings remain intact. The remaining $Nb_4(\mu_2\text{-}O(H))_4(\eta\text{-}O)_4$ ring partly opens to make the μ_2-O and η-O sites temporarily equivalent. At this point, the coordination number of each Nb(V) in the opening ring temporarily decreases from six to four or five (Figure 9) and isotopic exchange can be accomplished by reaction with a bulk water molecule. Note that this open structure is not centrosymmetric—the μ_6-O is ~3.6 Å from two of the Nb(V) and only ~2.1 Å from the remaining four Nb(V), to which it remains relatively tightly bound. This hypothesized opening of the Lindqvist structure must take place as a concerted motion involving all four sets of Nb(V) in a ring; exchange events at single metal sites were not computationally stable. This open metastable structure (Figure 9, bottom) is higher in energy by several tens of kJ/mol than the stable Lindqvist structure, as indicated by ab initio calculations at the B3LYP/DGDZVP/DFT level of theory using the COSMO continuum model for solvation.[30] (Different energies result from different overall stoichiometries and the assumed positions of the protons on the molecules.)

We hypothesize that a metastable form of the molecule, perhaps resembling in some fashion the structure in Figure 9, allows the η-O and μ_2-O(H) sites to become temporarily equivalent. At this point, the Nb(V) sites are coordinatively unsaturated and can easily accept an incoming water molecule. Once exchange is accomplished, it is irrelevant whether the rotation continues to completely interchange the η-O and μ_2-O(H) oxygens, or if the open structure reverses and collapses back into the original configuration. The important points are that this structure is present at low concentrations as a metastable fluctuation of the stable structure, that the oxygens become equivalent, and that the Nb(V) becomes temporarily coordinatively unsaturated and able to accept an incoming oxygen from H_2O. Formation of the metastable intermediate obviously reflects changes in reactivity with protonation, as indicated by the rate law (eq 4).

A mechanism that makes the two types of exchanging oxygens temporarily equivalent cannot fully explain the kinetic data, regardless of which structure is chosen as an intermediate, because there are twice as many bridging than terminal oxo sites. In the hypothetical open structure shown in Figure 9, for example, there is a higher proportion of terminal oxygens in the opening $Nb_4(\mu_2\text{-}O(H))_4(\eta\text{-}O)_4$ rings than in the bulk $[H_xNb_6O_{19}]^{(8-x)-}$ structure. The bulk structure has a ratio of $(\mu_2\text{-}O(H))/(\eta\text{-}O) = 2$ and the $Nb_4(\mu_2\text{-}O(H))_4(\eta\text{-}O)_4$ rings have $(\mu_2\text{-}O(H))/(\eta\text{-}O) = 1$. Thus, the fraction of terminal oxygens in the stable Lindqvist ion would be observed to exchange twice as fast as bridges, even if the two sites are periodically made equivalent by forming this $Nb_4(\mu_2\text{-}O(H))_4(\eta\text{-}O)_4$ structure. This hypothesis that the Lindqvist ion forms a metastable structure, although inadequate to explain all of the data, is consistent with other work on polyoxometalates that indicates pathways can involve more open metastable forms of the ion.[2,31−32]

The activation parameters (Table 2) are not fully consistent with a model where the oxygens become chemically equivalent. There are two types of coincidence to discuss. First, the data in Table 2 correspond to two different pH conditions and may include contributions from different protonated forms of the molecule, as discussed above. Second, and more importantly, the $\Delta H^{\ddagger}$ values should be the same if the exchange pathway that we suggest, an intermediate with temporary chemical equivalency of the two oxygens, accounts for the rate equivalency. Clearly the $\Delta H^{\ddagger}$ values for the two oxygens are virtually identical ($\Delta H^{\ddagger} \approx 90$ kJ/mol) at one condition (pH = 13) but are different at high pH (pH = 14.5; $\Delta H^{\ddagger} \approx 96$ and 107 kJ/mol). It is unfortunate that the molecule is so basic that a wider range of measurements at higher pH conditions are not possible. The large entropies are consistent with the separation of charges to make this expanded intermediate and the associated changes in solvation.

Any pathway where μ_2-O(H) and η-O sites become equivalent is obviously superseded in the region $11 < pH < 14$ where the rates of exchange of the η-O and μ_2-O(H) sites differ considerably. At these conditions, the dominant aqueous form is the monoprotonated $[HNb_6O_{19}]^{7-}$ ion (Figure 2), with the proton on a bridge, and the η-O sites react more slowly by a factor of ~10 than the μ_2-O(H) sites. Although the η-O sites react at rates that are virtually independent of pH in this region, there is a slight, but distinct, pH dependence to the rates of isotopic equilibration of the μ_2-O(H) that is particularly evident as pH exceeds pK_{a1} (pH > 13.6) and as it approaches pK_{a2} (pH < 11). At these pH conditions, one can see that the dominant speciation alters so that there is an appreciable fraction of $[Nb_6O_{19}]^{8-}$ and $[H_2Nb_6O_{19}]^{6-}$ ions, respectively. We do not know why the metastable opening of the Lindqvist ion (Figure 9) should be slow relative to another pathway when there is a single bridging μ_2-O(H), but this problem is well poised for simulation.

5. Conclusions

The rates of exchange of η-O and μ_2-O(H) sites in the hexaniobate anion with bulk solution differ considerably with pH. The pH dependency can be explained by appealing to changes in the protonation state of the molecule as a function of pH; no involvement of isotopically normal OH^-(aq) or H_3O^+(aq) is necessary. We find evidence for at least two conspicuous pathways for oxygen-isotopic exchange between η-O and μ_2-O(H) sites in the hexaniobate anion and bulk solution. When the dominant form of the molecule is a singly protonated $[HNb_6O_{19}]^{7-}$ ion, the reactivities of the η-O and μ_2-O(H) sites are distinctly different and the exchange rates of the η-O sites, but not the μ_2-O(H) sites, are virtually independent of pH. More interesting is a second pathway where isotopic exchange varies with pH and the η-O and μ_2-O(H) sites react at approximately equal rates, for reasons that we do not fully understand.

We suggest that a metastable form of the Lindqvist ion structure exists where the terminal and bridging oxygens are temporarily equivalent, but such a structure can only partly account for the kinetic results. Such a structure can be optimized ab initio as one of the $Nb_4(\mu_2\text{-}O(H))_4(\eta\text{-}O)_4$ rings opens. We hypothesize that, when the two oxygen sites become equivalent in this metastable structure, water reacts with the temporarily coordinatively undersaturated Nb(V). Equivalence of the η-O and μ_2-O(H) sites during isotopic exchange is most evident when the $[H_xNb_6O_{19}]^{(8-x)-}$ ion is protonated by 2−3 protons. A

(30) Frisch, M. J.; et al. *Gaussian 03*, revision C.02; Gaussian, Inc.: Wallingford, CT, 2004.
(31) Comba, P.; Helm, L. *Helv. Chim. Acta* **1988**, *71*, 1406.
(32) Hill, C. T. *Comprehensive Coordination Chemistry-II*; Elsevier: New York, 2004; Vol. 4, p 679.

metastable structure with equivalent oxygens may also be active when the ion is fully deprotonated as well, but we have too few data at the highest pH to conclude that the oxygens remain similarly reactive as the molecule becomes fully deprotonated. Our experience with the aluminum polyoxocations in the ϵ-Keggin structure[3] is that little can be learned without data on isostructural versions of the molecule and, fortunately, the Lindqvist ion structure allows for a wide range of such substitutions.

The fact that the entire pH variation in rates could be accounted for by changes in protonation state of the hexaniobate ion, without appealing to reaction with isotopically normal OH^- or H_3O^+, suggests that work on the polyoxometalate ions might be of considerable help to geochemists trying to understand similar reactions at oxide mineral surfaces. If we were to treat the hexaniobate ion as an oxide surface in water, we would find a rate law that shows bond ruptures to the proton-charge density, as is commonly observed for oxides in water.[28] None of the molecular detail, however, would be apparent in structures that are more complicated than this simple polyoxoanion, where reactions at individual oxygens can be followed explicitly.

Acknowledgment. We thank Prof. Jim Rustad for stimulating discussions. This research was supported by the U.S. DOE Office of Basic Energy Sciences via grant DE-FG03-02ER15325 to W.H.C. and the US NSF via EAR 0515600. Support for M.N. was from Sandia National Laboratories LDRD program. Sandia National Laboratories is a multiprogram laboratory operated by Sandia Corporation, A Lockheed Martin Company, for the U.S. DOE under contract DE-AC04-94Al85000. Spectrometers at the U.C. Davis NMR facility were purchased using funds from NSF grant OSTI 97-24412.

Supporting Information Available: Complete ref 30 and table of energies for optimized structures. This material is available free of charge via the Internet at http://pubs.acs.org.

JA065529W